

SNAD Transient Miner: Finding Missed Transient Events in ZTF DR4 using k-D trees

P. D. Aleo^{a,b}, K. L. Malanchev^{a,c}, M. V. Pruzhinskaya^c, E. E. O. Ishida^d,
E. Russeil^d, M. V. Kornilov^{c,e}, V. S. Korolev^{f,g}, S. Sreejith^h, A. A. Volnovaⁱ,
G. S. Narayan^{a,j}

^a*Department of Astronomy, University of Illinois at Urbana-Champaign, 1002 West Green Street, Urbana, 61801, IL, USA*

^b*Center for AstroPhysical Surveys (CAPS) Fellow, National Center for Supercomputing Applications, USA*

^c*Lomonosov Moscow State University, Sternberg Astronomical Institute, Universitetsky pr. 13, Moscow, 119234, Russia*

^d*Université Clermont Auvergne, CNRS/IN2P3, LPC, Clermont-Ferrand, F-63000, France*

^e*National Research University Higher School of Economics, 21/4 Staraya Basmannaya Ulitsa, Moscow, 105066, Russia*

^f*Central Aerohydrodynamic Institute, 1 Zhukovskiy st, Zhukovskiy, Moscow Region, 140180, Russia*

^g*Moscow Institute of Physics and Technology, 9 Institutskiy per., Dolgoprudny, Moscow Region, 141701, Russia*

^h*Physics Department, Brookhaven National Laboratory, Upton, NY, 11973, USA*

ⁱ*Space Research Institute of the Russian Academy of Sciences (IKI), 84/32 Profsoyuznaya Street, Moscow, 117997, Russia*

^j*Center for AstroPhysical Surveys (CAPS), National Center for Supercomputing Applications, 1205 West Clark Street, Urbana, 61801, IL, USA*

Abstract

We report the automatic detection of 11 transients (7 possible supernovae and 4 active galactic nuclei candidates) within the Zwicky Transient Facility fourth data release (ZTF DR4), all of them observed in 2018 and absent from public catalogs. Among these, three were not part of the ZTF alert stream. Our transient mining strategy employs 41 physically motivated features extracted from both real light curves and four simulated light curve models (SN Ia, SN II, TDE, SLSN-I). These features are input to a k-D

Email address: paleo2@illinois.edu (P. D. Aleo)

tree algorithm, from which we calculate the 15 nearest neighbors. After pre-processing and selection cuts, our dataset contained approximately a million objects among which we visually inspected the 105 closest neighbors from seven of our brightest, most well-sampled simulations, comprising 89 unique ZTF DR4 sources. Our result illustrates the potential of coherently incorporating domain knowledge and automatic learning algorithms, which is one of the guiding principles directing the **SNAD** team. It also demonstrates that the ZTF DR is a suitable testing ground for data mining algorithms aiming to prepare for the next generation of astronomical data.

Keywords: Transient sources (1851), Time domain astronomy (2109), Supernovae (1668), Active galactic nuclei (16)

PACS: 0000, 1111

2000 MSC: 0000, 1111

1. Introduction

The volume and complexity of astronomical data have drastically increased with the arrival of large scale astronomical surveys, the state of the art being the Zwicky Transient Facility¹ (ZTF), which generates ~ 1.4 TB of data per night of observation (Graham et al., 2019). This new data paradigm has forced astronomers to search for automatic tools which can enable classification and discovery within such large datasets.

Traditional supervised machine learning algorithms rely on the availability of large representative training samples, which are not feasible in astronomy (Ishida, 2019). Classification requires spectroscopic confirmation, which is an expensive and time consuming process. Given the advent of large scale photometric astronomical surveys, the community has devoted significant resources to systematic spectroscopic follow up of transient candidates. Initiatives like the Young Supernova Experiment (YSE, Jones et al., 2021), the Bright Transient Survey (BTS, Fremling et al., 2020) and the Global Supernova Project (Howell, 2019) aim to spectroscopically confirm a large number of candidates, which can latter be used as training sets for machine learning applications. Such efforts resulted in a significant increase in the number of available classifications in the last few years. Despite this important advancement, spectroscopic confirmation continues to be a rare

¹<https://www.ztf.caltech.edu/>

commodity due to the impossibility to follow-up all discovered photometric transients. Moreover, observations conditions required by spectroscopy limit the completeness of such samples for fainter sources, leaving a large fraction of photometrically observed candidates without proper classification.

In this context, the use of machine learning algorithms opens the possibility of studying larger populations within each class as well as their application in further scientific analysis. A particularly well-studied example of this scenario is the task of supernova (SN) photometric classification. Since their first use as standardizable candles (Riess et al., 1998; Perlmutter et al., 1999) a lot of effort has been devoted to the development, and adaptation, of machine learning classifiers which may enable purely photometric supernova cosmology (see Ishida, 2019, and references therein). This covers a large variety of learning algorithms (e.g. Lochner et al., 2016; Boone, 2019; Sooknunan et al., 2021; Alves et al., 2021), including deep (e.g., Muthukrishna et al., 2019; Pasquet et al., 2019; Möller et al., 2020; Villar et al., 2020; Allam and McEwen, 2021; Burhanudin et al., 2021) and adaptive (e.g., Ishida et al., 2019; Kennamer et al., 2020) learning techniques. These deep learning approaches leverage recurrent neural networks (RNNs, Muthukrishna et al., 2019; Möller et al., 2020), RNN-based autoencoders (Sadeh, 2020; Villar et al., 2021), Temporal Convolutional Networks (TCNs, Muthukrishna et al., 2021), and more.

This new direction towards data driven approaches has also benefited from increasingly more realistic simulations. Given the sparse availability of confirmed classifications, simulations have filled the gap when real data are not available. They have been used to compare results from different classifiers in the context of data challenges, like SNPhotCC (Kessler et al., 2010) and PLAsTiCC (Hložek et al., 2020), as well as used to replace training samples in transfer learning scenarios (e.g., Pasquet et al., 2019). In all such attempts, large volumes of simulations are used to infer statistical properties of different classes which can allow bulk data classification. In parallel, unsupervised learning techniques have been used for clustering (e.g., Krone-Martins and Moitinho, 2014; Ralph et al., 2019; Pera et al., 2021) and anomaly detection (e.g., Villar et al., 2020; Storey-Fisher et al., 2021; Martínez-Galarza et al., 2021; Lochner and Bassett, 2021) without the need of labels. In this context, simulations have also been used to validate the proposed algorithms (e.g., Villar et al., 2021).

The **SNAD**² team has been continuously working in the development of anomaly detection algorithms which are able to prove their efficiency in real data while incorporating domain knowledge in the machine learning model – thus tailoring it according to the scientific interest of the expert (e.g., Pruzhinskaya et al., 2019; Aleo et al., 2020; Malanchev et al., 2021; Ishida et al., 2021). In this work, we present a hybrid approach for mining transients in large astronomical datasets, specifically ZTF DR4; moreover, our methodology can also be applied to the nightly ZTF alert-stream via time-domain brokers like ANTARES (Matheson et al., 2021) and FINK (Möller et al., 2021). Ultimately, our analysis still focuses on performance on real data; however, we use a few simulated light curves as a guide to identify transients in a large dataset mostly comprised of variable stars (Chen et al., 2020).

We describe the data, simulations, and pre-processing steps in Section 2. The simulation-to-data matching algorithm is described in Section 3 and results are shown in Section 4. Our conclusions are outlined in Section 5.

2. Data

2.1. ZTF DR4

ZTF is a northern sky survey stationed at Mount Palomar. It uses a 48-inch Schmidt telescope equipped with a 47 deg² camera, with primary science objectives including the physics of SN and relativistic explosions, multi-messenger astrophysics, SN cosmology, active galactic nuclei (AGN), tidal disruption events (TDE), stellar variability and Solar System objects (Graham et al., 2019). The survey started on March 2018 and, during its initial phase, has observed around a billion objects (Bellm et al., 2019) in three photometric bands: ZTF-*g*, ZTF-*r*, ZTF-*i*. It is employed as a testing ground for the next generation of large scale surveys like the Vera Rubin Observatory Legacy Survey of Space and Time (LSST, LSST Science Collaboration et al. 2009). For this work, we use the survey’s fourth data release (DR4), made public on December 9, 2020³. In this work we use the two bluer filters, ZTF-*r* and ZTF-*g*, and denote them as *zr*– and *zg*–.

²<https://snad.space/>

³https://web.ipac.caltech.edu/staff/fmasci/ztf/dr4/ZTF_DR4.pdf

2.2. Simulations

We create realistic ZTF simulations using SNANA (Kessler et al., 2009), a catalog-level light curve simulator which includes effects due to telescope characteristics and observational conditions. We adopt ZTF data release 3 cadence and magnitude error distribution (see Chatterjee et al. 2021 for details). Starting from the template models originally developed for the Photometric LSST Astronomical Time-series Classification Challenge (PLAsTiCC, Kessler et al., 2019; Hložek et al., 2020), we selected those whose light curve were clearly non-periodic and/or with largest probability of being detected (high intrinsic brightness). Thus, our final model sample contained only SN Ia, SN II, SLSN-I, and TDE.

For each model, we generated $\sim 50,000^4$ simulations and imposed a series of quality cuts (SNR > 5 , magnitude limit, $m < 21.5^m$, and a minimum of 100 observations in each of the $zr-$ and $zg-$ bands). We then chose, among the surviving objects, the seven brightest light curves (3 SLSN-I, 1 SN Ia, 1 SN II and 2 TDE with peak magnitude $\sim 17^m$) and used these objects as input to our k-D tree (see Section 3). An example of a ZTF SN Ia simulation is given in Fig. 1.

2.3. Light curve selection

ZTF DR4 includes a photometric dataset grouped into objects by a detection position, an observation field, and a passband. Thus, a single stellar source can be represented by multiple objects due to overlapping fields and several observed passbands. We perform $0.2''$ cross-matching to associate different objects as a single source using the ClickHouse database management system⁵. We select observations with `catflags` = 0, positive `magerr`, in $zg-$ & $zr-$ passbands only, and within the first 420 days of the survey. Moreover, we consider objects with the absolute value of the galactic latitude larger than 15 degrees and having at least 100 detections per passband (non-detections are not presented in ZTF DRs). Finally, we filter out light curves having small variability for which $\frac{1}{N-1} \sum (\frac{m_i - \bar{m}}{\sigma_i})^2 < 3$, where N is the number of observations, m_i and σ_i are detection magnitudes and corresponding error estimates, and $\bar{m} \equiv \sum (m_i / \sigma_i^2) / \sum (1 / \sigma_i^2)$ is a weighted mean magnitude. As a result, we were left with 990,220 sources.

⁴This number results in a small but sufficient portion of well-sampled simulations located in the bright tail of the peak magnitude distribution.

⁵<https://clickhouse.com>

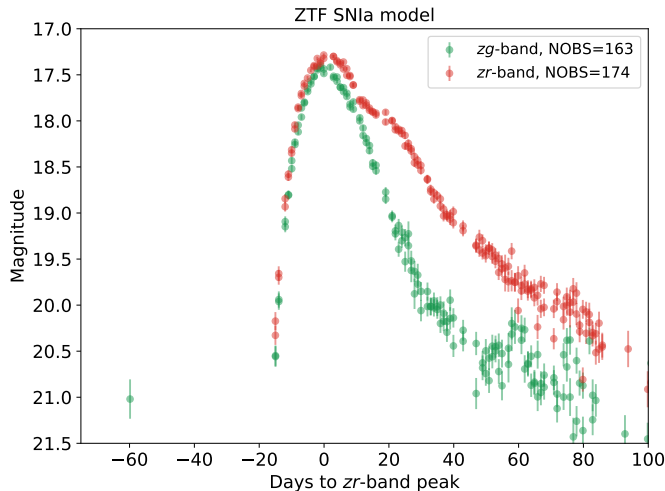


Figure 1: SNANA simulation of an SN Ia used to match with ZTF DR4 data. Green and red circles correspond to zg - and zr -band observations, respectively. Both bands have more than 100 detections with $\text{SNR} > 5$. This simulation’s tenth nearest neighbor via the k-D tree algorithm is SNAD156/AT 2018lzb.

2.4. Pre-processing

We extract light curve features for both simulations and our sample of ZTF DR4 data with the `light-curve`⁶ package (Malanchev et al., 2021). We use a total of 82 light curve features without scaling or normalization (41 per band) including magnitude amplitude, Stetson K coefficient (Stetson, 1996), standard deviation of Lomb-Scargle periodogram (Lomb, 1976a; Scargle, 1982a), etc. Our list encloses 68 magnitude-based and 14 flux-based features, whereby 66 are brightness-related and 16 are temporally-related; see the complete list in Appendix B.

3. Methodology

We take seven of the brightest simulations (3 SLSN-I, 1 SN Ia, 1 SN II and 2 TDE with peak magnitude $\sim 17^m$) and apply a k-D tree (Bentley, 1975) to their extracted 82 non-normalized features.⁷ Subsequently, we identify the

⁶<https://github.com/light-curve>

⁷Generally, feature scaling can be used to ensure all single-dimensional distances map to the same range of values. This is done in order to equally weight the calculation of

15 nearest neighbors for each simulation (105 matches in total, resulting in 89 unique ZTF DR4 sources). We chose to only inspect the first 15 nearest neighbors because it enables a sufficient test of the method’s validity while providing a manageable number of light curves to visually examine.

We inspected their light curves using the **SNAD ZTF viewer**⁸ (Malanchev et al., 2021), a tool that allows easy access to the individual exposure images; to the Aladin Sky Atlas (Bonnarel et al., 2000; Boch and Fernique, 2014); and to various catalogues of variable stars and transients, including the General Catalogue of Variable Stars (GCVS, Samus’ et al. 2017), the American Association of Variable Star Observers’ Variable Star Index (AAVSO VSX, Watson et al. 2006), the Asteroid Terrestrial-impact Last Alert System (ATLAS, Heinze et al. 2018), the ZTF Catalog of Periodic Variable Stars (Chen et al., 2020), *astrocats*⁹, the OGLE-III On-line Catalog of Variable Stars (Soszynski et al., 2008), and the SIMBAD database (Wenger et al., 2000). It also contains the information about object colour and galactic extinction in the chosen direction. Thus, we consider that all publicly available sources were included in our search. If an object was not announced by a survey, we consider it as undiscovered.

The k-D tree takes ~ 4 seconds on a 2 GHz Quad-Core Intel Core i5 processor. Although we use the default Euclidean distance metric for distance, we will explore other distance metrics such as Manhattan and Mahalanobis distances in future work.

The large dimension of the resulting parameter space is prone to produce non-optimal efficiency when presented to the k-D tree algorithm (curse of dimensionality). This is especially important when there is some correlation among the features (see Malanchev et al., 2021, Figure A.3). In order to access the performance of our method in a lower dimension parameter space, we also perform a similar analysis using a principal component analysis (PCA, Jolliffe, 2013) approach and compare results with those obtained from the complete feature set (see Section 5).

k-D distances across all features. In our case, the chosen feature set already meets this condition. In trying to apply the same method for another feature set, the reader should be aware of this condition.

⁸<https://ztf.snad.space/>

⁹<https://astrocats.space/>

Table 1: Results of transient mining in ZTF DR4 using k-D trees.

Name	R.A.	Dec.	Host galaxy*	z_{ph}	TNS	Type [†]	Comments
SNAD149	284.35219	67.17743			AT 2018lyu	PSN	ZTF18abrlhnm
SNAD150	240.75660	32.64360	SDSS J160301.52+323835.8		AT 2018lyv	PSN	ZTF18aaqnsia
SNAD151	190.61613	52.77285	SDSS J124227.87+524621.9	0.20±0.11	AT 2018lyw	PSN	ZTF19aaoykyz
SNAD152	212.40042	55.95669	SDSS J140936.12+555724.5	0.11±0.03	AT 2018lyx	PSN	ZTF18aanaryv
SNAD153	325.96473	24.35382	SDSS J214351.53+242113.6	0.17±0.04	AT 2018lyy	AGN	ZTF18abvosry
SNAD154	219.40247	38.04782	SDSS J143736.57+380252.0	0.22±0.08	AT 2018lyz	AGN	
SNAD155	212.29492	38.70615	SDSS J140910.77+384222.1	0.39±0.06	AT 2018lza	AGN	ZTF18acwyyib
SNAD156	184.83691	45.49015	SDSS J121920.85+452924.4	0.09±0.02	AT 2018lzb	PSN	
SNAD157	280.69720	36.36783			AT 2018lzc	PSN	ZTF18abegwmh
SNAD158	253.15763	25.82260	SDSS J165237.84+254921.2	0.14±0.05	AT 2018lzd	AGN	
SNAD159	216.86359	53.08862	SDSS J142727.25+530518.9	0.17±0.07	AT 2018lze	PSN	ZTF19aanjzps

* If available, candidate host galaxies from SDSS DR16 (Ahumada et al., 2020) and their corresponding photometric redshifts (z_{ph}).

† PSN — possible supernova, AGN — active galactic nucleus.

4. Results

4.1. Supernova and AGN candidates

As a result of transient mining, we discovered 11 previously unreported supernova and active galactic nucleus candidates (see Table 1). The remaining 94 matches (81 unique ZTF DR4 sources) were either known/already reported transients or variable stars. The full breakdown of all uniquely-matched source objects is presented in Table 2. We note that $\sim 50\%$ of our matched sources are variable stars (44), and 18 were transients. Given the large number of variable stars previously estimated in ZTF data releases (Chen et al., 2020), and our imposed selection cuts (see Section 2.3), it is reasonable to expect that a large fraction of our data set is composed of well sampled, high-amplitude variable stars whose coverage in parameter space significantly overlaps with the regions populated by transients (see, e.g. Figure 4). Thus, a ratio of 18 transients (11 newly-discovered) to 44 variable stars out of 89 unique sources selected from 990,220 considered ZTF sources is a very successful result. Considering the extreme case where ≈ 3000 SNe discovered by ZTF (Dhawan et al., 2022) were part of our data set, the expected incidence of SNe when choosing 100 sources at random would be of < 1 (≈ 0.3) event.

Table 3 shows a further breakdown of these 18 transients, detailing the 7 previously known and 11 SNAD-discovered transients from this paper, as well as the k -nearest neighbours match to its simulation type. Although we

Table 2: Total uniquely-matched ZTF DR4 sources, first 15 k -nearest neighbors.

Matched Source Type (count)	Subtype(s) (count)/Other notes
Variable Star (44)	RR Lyrae (27), UG (10), Mira (3), Semi-Regular (2), Cepheid (1), RS CVn (1)
Quasi-stellar (15)	QSO (14), BL Lacertae (1)
Galaxy (3)	Seyfert (2), Radio source (1)
Transient [†] (18)	Reported w/ classification (2), Reported w/o classification (5), This work (11)
Uncatalogued (9)	
Artifact (0)	

[†] A breakdown of this category, including various demographics with nearest-neighbor and simulation type matches, can be found in Table 3.

cannot claim that every instance of model neighbor will define the class of the found transient (particularly when there are several model simulation types matched to a singular event, e.g. AT2019gsn, SNAD149, SNAD150, SNAD151), we note that in the two cases where the spectroscopic class was available, it did match the simulation class: SN2018aej, SN2018aoy. Any possible correlation will be explored in future work.

Among the 11 new objects, 9 are coincident with galaxy positions cataloged in SDSS DR16 (Ahumada et al., 2020), thus confirming their extragalactic origin. We conclude that 7 of the candidates are likely to be SNe and 4 others are AGN candidates (see Fig. A.5). All candidates were sent to the Transient Name Server¹⁰ (TNS) and received an official TNS identifier as well as an internal SNAD name (Table 1).

Among our discovery objects, SNAD150, SNAD152, and SNAD155 occurred when the ZTF template reference image was taken. This detail provides a possible reason for why they were initially unreported, as the ZTF alert stream utilizes differential photometry, and typically the science image contains the transient, whereas here the reference image contains the transient. Perhaps more importantly, another three objects from our list are missing in the official ZTF alert stream, two of which we classify as AGN candidates (SNAD154, SNAD158) and the third as a possible SN (SNAD156). Using the SNAD viewer, we investigated the placement of all newly discovered transients in the original FITS files, in order to confirm if this could be a result of missing reference image in chip-edges. We found that SNAD155 and SNAD159 are indeed placed somewhat close to image borders, but those are not the objects

¹⁰<https://www.wis-tns.org/>

Table 3: Transient demographics among the first 15 k -nearest neighbors.

Name/TNS	k -nearest neighbor	Previously Known?	Matched Simulation	Class (if known)
ATLAS20hzm/AT 2019mzp	$k=2$	Yes	SLSN-I	
ATLAS19mbr/AT 2019gsn	$k=3$	Yes	SN II	
"	$k=5$		TDE	
"	$k=8$		SN Ia	
"	$k=8$		SLSN-I	
SNAD129/AT 2018lxn	$k=9$	Yes	SN Ia	
ATLAS18oay/AT 2018bhq	$k=12$	Yes	TDE	
PS18mh/SN 2018aej	$k=13$	Yes	SN Ia	SN Ia
ZTF19aaqejgh/AT 2018dvs	$k=14$	Yes	SN Ia	
ATLAS18mzo/SN 2018aoy	$k=14$	Yes	SN Ia	SN Ia
SNAD149/AT 2018lyu	$k=2$	No	TDE	
"	$k=12$		SLSN-I	
SNAD150/AT 2018lyv	$k=4$	No	TDE	
"	$k=5$		SN Ia	
"	$k=6$		SLSN-I	
SNAD151/AT 2018lyw	$k=6$	No	TDE	
"	$k=8$		SN Ia	
SNAD152/AT 2018lyx	$k=2$	No	SN Ia	
SNAD153/AT 2018lyy	$k=6$	No	TDE	
SNAD154/AT 2018lyz	$k=13$	No	TDE	
SNAD155/AT 2018lza	$k=9$	No	TDE	
SNAD156/AT 2018lzb	$k=10$	No	SN Ia	
SNAD157/AT 2018lzc	$k=11$	No	SN Ia	
SNAD158/AT 2018lzd	$k=14$	No	SN II	
SNAD159/AT 2018lze	$k=15$	No	SN II	

Note: Only unique matches have their official name listed. Additional (duplicate) matches for any particular source is subsequently denoted by quotation marks.

absent in the alert stream. Missed transients **SNAD154** and **SNAD156** have a peak magnitude $\sim 18.5^m - 19.5^m$ which is comparable to those of other SNAD objects listed here but are also detected by the alert system. Moreover, some of our candidates (e.g., **SNAD150**, **SNAD151**) have well-sampled early light curves which could help constrain the progenitor parameters of supernovae and shed light on the explosion scenarios (Jones et al., 2021).

To illustrate the scientific significance of these candidates, we perform light curve fits on two of them, **SNAD150** and **SNAD154**. We use the PYTHON library `SNCOSMO`¹¹ to fit their light curves with Peter Nugent’s spectral templates¹² which cover the main supernova types (Ia, Ib/c, IIP, IIL, IIn). Nugent’s models are simple spectral time series that can be scaled up and down. The zero phase is defined relative to the explosion moment and the observed time t is related to phase via $t = t_0 + \text{phase} \times (1+z)$. Other model parameters are redshift z , observer-frame time corresponding to the zero source’s phase t_0 , and the amplitude.

We extract photometry in $zg-$, $zr-$, and $zi-$ passbands from only one field. Then, we subtract the reference magnitude from ZTF light curves to roughly account for the host galaxy contamination. To estimate the redshift bounds for **SNAD150**, we adopt $[-15; -22]$ as an acceptable region for the supernovae absolute magnitude (Richardson et al., 2014) and then, using the apparent maximum magnitude, transform it to the possible redshift range. For **SNAD154** there is a known SDSS galaxy at the source position with measured photometric redshift and corresponding errors, which we use for redshift bounds. Results of the fit are shown in Figs. 2 and 3. **SNAD150** light curves are best described by Nugent’s Type Ia Supernova model, while **SNAD154** is not well fitted by any of them—the observed light curve width near the peak brightness in zg and zr bands is smaller than the models suggest. Thus, we conclude that **SNAD154** object is likely to be an active galactic nucleus.

4.2. Feature space examination

We also investigate the effectiveness of simple data-quality cuts in discovering the SNAD transients listed in this work, when compared to the results obtained from the complete pipeline using an heuristic search. Using the

¹¹<https://sncosmo.readthedocs.io/en/stable/>

¹²https://c3.lbl.gov/nugent/nugent_templates.html

assumption that such transients could be found by selecting the highest-amplitude objects among a relatively bright population (peak magnitude $\sim 18^m$), we selected all objects fulfilling three criteria in both zg - and zr -light curves:

1. *error-weighted mean magnitude* $\in (18^m; 21^m)$, which removes bright and faint light curves with few bright outlier observations,
2. the highest *Lomb–Scargle periodogram peak power to the power standard deviation ratio* < 10 , which removes light curves showing periodicity,¹³
3. light curve *magnitude amplitude* $> 1.75^m$.¹⁴

After visually inspecting 105 objects resulting from this heuristic search, we found no supernova-like or AGN-like light curves. In fact, most of the objects present artifacts or are standard eruptive and cataclysmic variables.

Figure 4 shows that cuts in magnitude feature space (here we used zg -band *magnitude amplitude* and zg -band *error-weighted mean magnitude*) are not able to isolate our SNAD transients from the rest of the ZTF DR4 sample, including the region of feature space probed by the heuristic search. In fact, even if one *a priori* knew the magnitude mean and amplitude ranges to look for such transients, there would be an overwhelming amount of other variable stars, QSOs, and other non-transient phenomena among the ZTF DR4 objects to inspect. Considering the density of total sources in the *magnitude amplitude* $\in [0.7; 1.7]$, *error-weighted mean magnitude* $\in [19^m; 21^m]$ region, it is unlikely that one would retrieve our discovered SNAD transients without the machine learning part of the pipeline.

5. Conclusions

The consequences of large and complex astronomical datasets have been extensively discussed in the literature. A large part of such discussions focus on the potential of different machine learning algorithms, and are backed by their performance on large simulated datasets. This allows researchers to

¹³Some of the light curves could show bogus variability, e.g. ~ 1 day, so this criterion could remove some non-periodic sources.

¹⁴We chose this value to obtain a new set of 105 objects to visually inspect and compare against our 105 matched nearest-neighbors.

report on statistical properties of classifiers. In this work, we explored the potential of simulations from a different perspective.

Our analysis relies on two hypotheses: 1) state of the art simulations are a good proxy to real data, and 2) astrophysically inspired features correctly summarize the information necessary to characterize transient light curves. These hypotheses perfectly translate the underlying principles of all **SNAD** efforts, whose focus is to construct environments that coherently incorporate domain knowledge in learning strategies.

Both statements were tested by extracting the same 82 features from a small number of simulations (7 light curves representing 4 different classes) as well as from real data (ZTF DR4, comprising 990,220 objects). Subsequently, a k-D tree with Euclidean distance was used to search for the 15 objects in real data which were closest match in feature space to each simulation. By visually inspecting 105 total source matches (89 unique), we identified 11 previously unreported transient events, all occurring in 2018. Among these, 7 possible supernovae and 4 AGN candidates, the majority of them with light curves containing several observed epochs before maximum brightness.

We are aware that at 82 dimensions, the k-D tree suffers from the curse of dimensionality, and in general, using a k-D tree of k -dimensions to probe N points in a dataset should satisfy $N \gg 2^k$; otherwise, the efficiency of the search is no better than an exhaustive one (Kung et al., 2001). To this point, we are not aiming for the most efficient search algorithm, but an approach allowing us to find closest neighbours in the light-curve feature space. Moreover, because we only had 7 simulations to associate, our k-D tree search only takes ~ 4 seconds to run. To further investigate how the efficiency of our method is affected by the high number of features, we also performed the k-D tree analysis in a 15 dimension parameter space resulting from Principal Component Analysis (PCA, Jolliffe, 1986). This dimensionality reduction retains 86% of the variance of our original 82 dimensional parameter space. We obtained results in good agreement (Mira stars, cataclysmic variables, confirmed SN, unconfirmed transients, etc.) with those presented here, including some of the same discovery objects listed in this work (e.g. **SNAD150**). A detailed analysis of this lower dimensional parameter space and its quantitative impact on our results is an interesting investigation suited for subsequent work.

Beyond confirming our initial hypothesis about the importance of simulations and physically inspired features, such results also highlight the importance of further improving observation pipelines and the central role classical

learning algorithms can play in this task. Our candidates include 3 objects which were not part of the ZTF alert stream despite being as bright as the others and holding a considerable number of pre-maximum observations. Although currently it is not feasible to precisely determine why such candidates were lost, a few possible explanations include: the completeness of magnitude limited surveys for fainter sources, active transients when the template image was taken (which may explain **SNAD150**, **SNAD152** and **SNAD155**) or issues in the imaging pipeline. However, it is likely that the main reason behind the high fraction of non-identified transients ($\approx 12\%$, 11 new sources among 89 visually inspected) is the period of the data scrutinized in this work. All our sources were observed in 2018, when the ZTF ecosystem was in the beginning of its operations. It is reasonable to expect that a few transients were lost due to non-optimal pipeline parameters which were improved in subsequent years. We are currently working on applying the **SNAD** infrastructure to data from latter years to better understand how the fraction of non-reported transients vary with time. This will shed some light into the reasons behind the results presented in this paper and, at the same time, help prevent similar future losses. Given the importance of early observations in astrophysical investigations, this understanding is an important step towards an optimal exploitation of our observational resources.

Finally, we highlight the potential of ZTF DRs as a fertile ground for testing machine learning pipelines currently being prepared for future large scale surveys. Since we expect transient events to be a small fraction of the total number of objects in the DRs, it provides a perfect environment to stress-test data mining and anomaly detection algorithms, which do not require a large number of labels, before the arrival of LSST.

The era of big data in astronomy has imposed the necessity of automatic learning algorithms in order to digest large and complex datasets. Nevertheless, we should not underestimate the role of domain experts when adapting machines to work in real scientific data environments. Their input is vital to direct changes in the learning strategy due to the expert's response (e.g. as in active learning algorithms) or in the design of physically motivated features, realistic simulations and physically motivated evaluation criteria. The successful incorporation of this long acquired knowledge to automatic learning frameworks is necessary to ensure we will be able to fully explore the scientific potential of our data.

6. Acknowledgments

The authors thank Vasilisa Malancheva, Anastasia Malancheva, and Vadim Krushinsky for enlightening discussions. We would also like to thank Rick Kessler for his help with ZTF simulations and SNANA and the anonymous referee for comments that helped improved the clarity of the paper. The authors thank Jelena Banjac and Joé Veber for logistical help and hosting during the SNAD IV workshop, of which this work is a product.

The reported study was funded by RFBR and CNRS according to the research project № 21-52-15024. SNAD receives financial support from CNRS International Emerging Actions under the project *Real-time analysis of astronomical data for the Legacy Survey of Space and Time* during 2021-2022. The authors acknowledge the support by the Interdisciplinary Scientific and Educational School of Moscow University “Fundamental and Applied Space Research”. P.D.A. is supported by the Center for Astrophysical Surveys at the National Center for Supercomputing Applications (NCSA) as an Illinois Survey Science Graduate Fellow. This research also used resources of the National Energy Research Scientific Computing Center (NERSC), a U.S. Department of Energy Office of Science User Facility located at Lawrence Berkeley National Laboratory, operated under Contract No. DE-AC02-05CH11231. A.A.V. is supported by RSFC grant 18-12-00378 for anomalies light curves analysis.

This manuscript has been authored by employees of Brookhaven Science Associates, LLC under Contract No. DE-SC0012704 with the U.S. Department of Energy. The publisher by accepting the manuscript for publication acknowledges that the United States Government retains a non-exclusive, paid-up, irrevocable, world-wide license to publish or reproduce the published form of this manuscript, or allow others to do so, for United States Government purposes.

This research has made use of NASA’s Astrophysics Data System Bibliographic Services and following Python software packages: NUMPY (van der Walt et al., 2011), MATPLOTLIB (Hunter, 2007), SCIPY (Jones et al., 2001), PANDAS (pandas development team, 2020; Wes McKinney, 2010), SCIKIT-LEARN (Pedregosa et al., 2011), ASTROPY (Astropy Collaboration et al., 2013, 2018), and ASTROQUERY (Ginsburg et al.).

References

Ahumada, R., Allende Prieto, C., Almeida, A., et al., 2020. The 16th Data

- Release of the Sloan Digital Sky Surveys: First Release from the APOGEE-2 Southern Survey and Full Release of eBOSS Spectra. *ApJS* 249, 3. doi:10.3847/1538-4365/ab929e, arXiv:1912.02905.
- Aleo, P.D., Ishida, E.E.O., Kornilov, M., et al., 2020. The Most Interesting Anomalies Discovered in ZTF DR3 from the SNAD-III Workshop. *Research Notes of the American Astronomical Society* 4, 112. doi:10.3847/2515-5172/aba6e8.
- Allam, Tarek, J., McEwen, J.D., 2021. Paying Attention to Astronomical Transients: Photometric Classification with the Time-Series Transformer. arXiv e-prints , arXiv:2105.06178arXiv:2105.06178.
- Alves, C.S., Peiris, H.V., Lochner, M., McEwen, J.D., Allam, Tarek, J., Biswas, R., 2021. Considerations for optimizing photometric classification of supernovae from the Rubin Observatory. arXiv e-prints , arXiv:2107.07531arXiv:2107.07531.
- Astropy Collaboration, Price-Whelan, A.M., SipHocz, B.M., et al., 2018. The Astropy Project: Building an Open-science Project and Status of the v2.0 Core Package. *The Astronomical Journal* 156, 123. doi:10.3847/1538-3881/aabc4f, arXiv:1801.02634.
- Astropy Collaboration, Robitaille, T.P., Tollerud, E.J., et al., 2013. Astropy: A community Python package for astronomy. *Astronomy and Astrophysics* 558, A33. doi:10.1051/0004-6361/201322068, arXiv:1307.6212.
- Bellm, E.C., Kulkarni, S.R., Graham, M.J., et al., 2019. The Zwicky Transient Facility: System Overview, Performance, and First Results. *Publications of the Astronomical Society of the Pacific* 131, 018002. doi:10.1088/1538-3873/aaecbe, arXiv:1902.01932.
- Bentley, J.L., 1975. Multidimensional binary search trees used for associative searching. *Commun. ACM* 18, 509–517. URL: <https://doi.org/10.1145/361002.361007>, doi:10.1145/361002.361007.
- Boch, T., Fernique, P., 2014. Aladin Lite: Embed your Sky in the Browser, in: Manset, N., Forshay, P. (Eds.), *Astronomical Data Analysis Software and Systems XXIII*, p. 277.

- Bonnarel, F., Fernique, P., Bienaymé, O., et al., 2000. The ALADIN interactive sky atlas. A reference tool for identification of astronomical sources. *A&AS* 143, 33–40. doi:10.1051/aas:2000331.
- Boone, K., 2019. Avocado: Photometric Classification of Astronomical Transients with Gaussian Process Augmentation. *AJ* 158, 257. doi:10.3847/1538-3881/ab5182, arXiv:1907.04690.
- Burhanudin, U.F., Maund, J.R., Killestein, T., et al., 2021. Light-curve classification with recurrent neural networks for GOTO: dealing with imbalanced data. *MNRAS* 505, 4345–4361. doi:10.1093/mnras/stab1545, arXiv:2105.11169.
- Chatterjee, D., Narayan, G., Aleo, P.D., et al., 2021. El-CID: A filter for Gravitational-wave Electromagnetic Counterpart Identification. arXiv e-prints, arXiv:2108.04166arXiv:2108.04166.
- Chen, X., Wang, S., Deng, L., et al., 2020. The Zwicky Transient Facility Catalog of Periodic Variable Stars. *ApJS* 249, 18. doi:10.3847/1538-4365/ab9cae, arXiv:2005.08662.
- Dhawan, S., Goobar, A., Smith, M., Johansson, J., Rigault, M., Nordin, J., Biswas, R., Goldstein, D., Nugent, P., Kim, Y.L., Miller, A.A., Graham, M.J., Medford, M., Kasliwal, M.M., Kulkarni, S.R., Duev, D.A., Bellm, E., Rosnet, P., Riddle, R., Sollerman, J., 2022. The Zwicky Transient Facility Type Ia supernova survey: first data release and results. *MNRAS* 510, 2228–2241. doi:10.1093/mnras/stab3093, arXiv:2110.07256.
- D’Isanto, A., Cavuoti, S., Brescia, M., et al., 2016. An analysis of feature relevance in the classification of astronomical transients with machine learning methods. *Monthly Notices of the Royal Astronomical Society* 457, 3119–3132. doi:10.1093/mnras/stw157, arXiv:1601.03931.
- Fremling, C., Miller, A.A., Sharma, Y., Dugas, A., Perley, D.A., Taggart, K., Sollerman, J., Goobar, A., Graham, M.L., Neill, J.D., Nordin, J., Rigault, M., Walters, R., Andreoni, I., Bagdasaryan, A., Belicki, J., Cannella, C., Bellm, E.C., Cenko, S.B., De, K., Dekany, R., Frederick, S., Golkhou, V.Z., Graham, M.J., Helou, G., Ho, A.Y.Q., Kasliwal, M.M., Kupfer, T., Laher, R.R., Mahabal, A., Masci, F.J., Riddle, R., Rusholme, B., Schulze, S., Shupe, D.L., Smith, R.M., van Velzen, S., Yan, L., Yao, Y., Zhuang,

- Z., Kulkarni, S.R., 2020. The Zwicky Transient Facility Bright Transient Survey. I. Spectroscopic Classification and the Redshift Completeness of Local Galaxy Catalogs. *ApJ* 895, 32. doi:10.3847/1538-4357/ab8943, arXiv:1910.12973.
- Ginsburg, A., Sipócz, B.M., Brasseur, C.E., Cowperthwaite, P.S., et al., .
- Graham, M.J., Kulkarni, S.R., Bellm, E.C., et al., 2019. The zwicky transient facility: Science objectives. *Publications of the Astronomical Society of the Pacific* 131, 078001. URL: <https://doi.org/10.1088/1538-3873/ab006c>, doi:10.1088/1538-3873/ab006c.
- Heinze, A.N., Tonry, J.L., Denneau, L., et al., 2018. A First Catalog of Variable Stars Measured by the Asteroid Terrestrial-impact Last Alert System (ATLAS). *The Astronomical Journal* 156, 241. doi:10.3847/1538-3881/aae47f, arXiv:1804.02132.
- Hložek, R., Ponder, K.A., Malz, A.I., et al., 2020. Results of the Photometric LSST Astronomical Time-series Classification Challenge (PLAsTiCC). arXiv e-prints , arXiv:2012.12392arXiv:2012.12392.
- Howell, D., 2019. The Global Supernova Project, in: *American Astronomical Society Meeting Abstracts #233*, p. 258.16.
- Hunter, J.D., 2007. Matplotlib: A 2D Graphics Environment. *Computing in Science and Engineering* 9, 90–95. doi:10.1109/MCSE.2007.55.
- Ishida, E.E.O., 2019. Machine learning and the future of supernova cosmology. *Nature Astronomy* 3, 680–682. doi:10.1038/s41550-019-0860-6, arXiv:1908.02315.
- Ishida, E.E.O., Beck, R., González-Gaitán, S., et al., 2019. Optimizing spectroscopic follow-up strategies for supernova photometric classification with active learning. *MNRAS* 483, 2–18. doi:10.1093/mnras/sty3015, arXiv:1804.03765.
- Ishida, E.E.O., Kornilov, M.V., Malanchev, K.L., et al., 2021. Active anomaly detection for time-domain discoveries. *A&A* 650, A195. doi:10.1051/0004-6361/202037709, arXiv:1909.13260.

- Jolliffe, I., 2013. *Principal Component Analysis*. Springer Series in Statistics, Springer New York. URL: <https://books.google.fr/books?id=-ongBwAAQBAJ>.
- Jolliffe, I.T., 1986. *Principal Component Analysis and Factor Analysis*. Springer New York, New York, NY. pp. 115–128. URL: https://doi.org/10.1007/978-1-4757-1904-8_7, doi:10.1007/978-1-4757-1904-8_7.
- Jones, D.O., Foley, R.J., Narayan, G., et al., 2021. The Young Supernova Experiment: Survey Goals, Overview, and Operations. *ApJ* 908, 143. doi:10.3847/1538-4357/abd7f5, arXiv:2010.09724.
- Jones, E., Oliphant, T., Peterson, P., et al., 2001. SciPy: Open source scientific tools for Python. URL: <http://www.scipy.org/>. [Online; accessed `today`].
- Kenamer, N., Ishida, E.E.O., González-Gaitán, S., et al., 2020. Active learning with respect: Resource allocation for extragalactic astronomical transients, in: 2020 IEEE Symposium Series on Computational Intelligence (SSCI), pp. 3115–3124. doi:10.1109/SSCI47803.2020.9308300.
- Kessler, R., Bassett, B., Belov, P., et al., 2010. Results from the Supernova Photometric Classification Challenge. *PASP* 122, 1415. doi:10.1086/657607, arXiv:1008.1024.
- Kessler, R., Bernstein, J.P., Cinabro, D., et al., 2009. SNANA: A Public Software Package for Supernova Analysis. *PASP* 121, 1028. doi:10.1086/605984, arXiv:0908.4280.
- Kessler, R., Narayan, G., Avelino, A., et al., 2019. Models and Simulations for the Photometric LSST Astronomical Time Series Classification Challenge (PLAsTiCC). *PASP* 131, 094501. doi:10.1088/1538-3873/ab26f1, arXiv:1903.11756.
- Kim, D.W., Protopapas, P., Bailer-Jones, C.A.L., et al., 2014. The EPOCH Project. I. Periodic variable stars in the EROS-2 LMC database. *Astronomy and Astrophysics* 566, A43. doi:10.1051/0004-6361/201323252, arXiv:1403.6131.

- Krone-Martins, A., Moitinho, A., 2014. UPMASK: unsupervised photometric membership assignment in stellar clusters. *A&A* 561, A57. doi:10.1051/0004-6361/201321143, arXiv:1309.4471.
- Kung, S.Y., Larsen, J., Guan, L., 2001. Multimedia image and video processing / edited by Ling Guan, Sun-Yuan Kung, Jan Larsen. CRC Press Boca Raton, Fla.
- Lochner, M., Bassett, B.A., 2021. ASTRONOMALY: Personalised active anomaly detection in astronomical data. *Astronomy and Computing* 36, 100481. doi:10.1016/j.ascom.2021.100481, arXiv:2010.11202.
- Lochner, M., McEwen, J.D., Peiris, H.V., Lahav, O., Winter, M.K., 2016. Photometric Supernova Classification with Machine Learning. *ApJS* 225, 31. doi:10.3847/0067-0049/225/2/31, arXiv:1603.00882.
- Lomb, N.R., 1976a. Least-Squares Frequency Analysis of Unequally Spaced Data. *Ap&SS* 39, 447–462. doi:10.1007/BF00648343.
- Lomb, N.R., 1976b. Least-Squares Frequency Analysis of Unequally Spaced Data. *Astrophysics and Space Science* 39, 447–462. doi:10.1007/BF00648343.
- LSST Science Collaboration, Abell, P.A., Allison, J., et al., 2009. LSST Science Book, Version 2.0. ArXiv e-prints arXiv:0912.0201.
- Malanchev, K.L., Pruzhinskaya, M.V., Korolev, V.S., et al., 2021. Anomaly detection in the Zwicky Transient Facility DR3. *MNRAS* 502, 5147–5175. doi:10.1093/mnras/stab316, arXiv:2012.01419.
- Martínez-Galarza, J.R., Bianco, F.B., Crake, D., Tirumala, K., Mahabal, A.A., Graham, M.J., Giles, D., 2021. A method for finding anomalous astronomical light curves and their analogs. *MNRAS* doi:10.1093/mnras/stab2588, arXiv:2009.06760.
- Matheson, T., Stubens, C., Wolf, N., Lee, C.H., Narayan, G., Saha, A., Scott, A., Soraisam, M., Bolton, A.S., Hauger, B., Silva, D.R., Kececioglu, J., Scheidegger, C., Snodgrass, R., Aleo, P.D., Evans-Jacquez, E., Singh, N., Wang, Z., Yang, S., Zhao, Z., 2021. The ANTARES Astronomical Time-domain Event Broker. *AJ* 161, 107. doi:10.3847/1538-3881/abd703, arXiv:2011.12385.

- Wes McKinney, 2010. Data Structures for Statistical Computing in Python, in: Stéfan van der Walt, Jarrod Millman (Eds.), Proceedings of the 9th Python in Science Conference, pp. 56 – 61. doi:10.25080/Majora-92bf1922-00a.
- Möller, A., Peloton, J., Ishida, E.E.O., et al., 2020. Fink, a new generation of broker for the LSST community. arXiv e-prints , arXiv:2009.10185arXiv:2009.10185.
- Möller, A., Peloton, J., Ishida, E.E.O., Arnault, C., Bachelet, E., Blaineau, T., Boutigny, D., Chauhan, A., Gangler, E., Hernandez, F., Hrivnac, J., Leoni, M., Leroy, N., Moniez, M., Pateyron, S., Ramparison, A., Turpin, D., Ansari, R., Allam, Tarek, J., Bajat, A., Biswas, B., Boucaud, A., Bregeon, J., Campagne, J.E., Cohen-Tanugi, J., Coleiro, A., Dornic, D., Fouchez, D., Godet, O., Gris, P., Karpov, S., Nebot Gomez-Moran, A., Neveu, J., Plaszczyński, S., Savchenko, V., Webb, N., 2021. FINK, a new generation of broker for the LSST community. MNRAS 501, 3272–3288. doi:10.1093/mnras/staa3602, arXiv:2009.10185.
- Muthukrishna, D., Mandel, K.S., Lochner, M., Webb, S., Narayan, G., 2021. Real-time detection of anomalies in large-scale transient surveys. arXiv e-prints , arXiv:2111.00036arXiv:2111.00036.
- Muthukrishna, D., Narayan, G., Mandel, K.S., et al., 2019. RAPID: Early Classification of Explosive Transients Using Deep Learning. PASP 131, 118002. doi:10.1088/1538-3873/ab1609, arXiv:1904.00014.
- Pasquet, J., Pasquet, J., Chaumont, M., et al., 2019. PELICAN: deeP architecture for the LIght Curve ANalysis. A&A 627, A21. doi:10.1051/0004-6361/201834473, arXiv:1901.01298.
- Pedregosa, F., Varoquaux, G., Gramfort, A., et al., 2011. Scikit-learn: Machine learning in Python. Journal of Machine Learning Research 12, 2825–2830.
- Pera, M.S., Perren, G.I., Moitinho, A., et al., 2021. pyUPMASK: an improved unsupervised clustering algorithm. A&A 650, A109. doi:10.1051/0004-6361/202040252, arXiv:2101.01660.

- Perlmutter, S., Aldering, G., Goldhaber, G., et al., 1999. Measurements of Ω and Λ from 42 High-Redshift Supernovae. *ApJ* 517, 565–586. doi:10.1086/307221, arXiv:astro-ph/9812133.
- Pruzhinskaya, M.V., Malanchev, K.L., Kornilov, M.V., et al., 2019. Anomaly detection in the Open Supernova Catalog. *Monthly Notices of the Royal Astronomical Society* 489, 3591–3608. doi:10.1093/mnras/stz2362, arXiv:1905.11516.
- Ralph, N.O., Norris, R.P., Fang, G., et al., 2019. Radio Galaxy Zoo: Unsupervised Clustering of Convolutionally Auto-encoded Radio-astronomical Images. *PASP* 131, 108011. doi:10.1088/1538-3873/ab213d, arXiv:1906.02864.
- Richardson, D., Jenkins, Robert L., I., Wright, J., et al., 2014. Absolute-magnitude Distributions of Supernovae. *AJ* 147, 118. doi:10.1088/0004-6256/147/5/118, arXiv:1403.5755.
- Riess, A.G., Filippenko, A.V., Challis, P., et al., 1998. Observational Evidence from Supernovae for an Accelerating Universe and a Cosmological Constant. *AJ* 116, 1009–1038. doi:10.1086/300499, arXiv:astro-ph/9805201.
- Sadeh, I., 2020. Data-driven Detection of Multimessenger Transients. *ApJ* 894, L25. doi:10.3847/2041-8213/ab8b5f, arXiv:2005.06406.
- Samus', N.N., Kazarovets, E.V., Durlevich, O.V., et al., 2017. General catalogue of variable stars: Version GCVS 5.1. *Astronomy Reports* 61, 80–88. doi:10.1134/S1063772917010085.
- Sánchez, P., Lira, P., Cartier, R., Pérez, V., Miranda, N., Yovaniniz, C., Arévalo, P., Milvang-Jensen, B., Fynbo, J., Dunlop, J., Coppi, P., Marchesi, S., 2017. Near-infrared Variability of Obscured and Unobscured X-Ray-selected AGNs in the COSMOS Field. *ApJ* 849, 110. doi:10.3847/1538-4357/aa9188, arXiv:1710.01306.
- Scargle, J.D., 1982a. Studies in astronomical time series analysis. II. Statistical aspects of spectral analysis of unevenly spaced data. *ApJ* 263, 835–853. doi:10.1086/160554.

- Scargle, J.D., 1982b. Studies in astronomical time series analysis. II. Statistical aspects of spectral analysis of unevenly spaced data. *The Astrophysical Journal* 263, 835–853. doi:10.1086/160554.
- Sooknunan, K., Lochner, M., Bassett, B.A., Peiris, H.V., Fender, R., Stewart, A.J., Pietka, M., Woudt, P.A., McEwen, J.D., Lahav, O., 2021. Classification of multiwavelength transients with machine learning. *MNRAS* 502, 206–224. doi:10.1093/mnras/staa3873, arXiv:1811.08446.
- Soszynski, I., Poleski, R., Udalski, A., et al., 2008. The Optical Gravitational Lensing Experiment. The OGLE-III Catalog of Variable Stars. I. Classical Cepheids in the Large Magellanic Cloud. *Acta Astron.* 58, 163–185. arXiv:0808.2210.
- Stetson, P.B., 1996. On the Automatic Determination of Light-Curve Parameters for Cepheid Variables. *Publications of the Astronomical Society of the Pacific* 108, 851. doi:10.1086/133808.
- Storey-Fisher, K., Huertas-Company, M., Ramachandra, N., et al., 2021. Anomaly detection in Hyper Suprime-Cam galaxy images with generative adversarial networks. *MNRAS* doi:10.1093/mnras/stab2589, arXiv:2105.02434.
- pandas development team, T., 2020. pandas-dev/pandas: Pandas. URL: <https://doi.org/10.5281/zenodo.3509134>, doi:10.5281/zenodo.3509134.
- van der Walt, S., Colbert, S.C., Varoquaux, G., 2011. The NumPy Array: A Structure for Efficient Numerical Computation. *Computing in Science and Engineering* 13, 22–30. doi:10.1109/MCSE.2011.37, arXiv:1102.1523.
- Villar, V.A., Cranmer, M., Berger, E., Contardo, G., Ho, S., Hosseinzadeh, G., Lin, J.Y.Y., 2021. A Deep-learning Approach for Live Anomaly Detection of Extragalactic Transients. *ApJS* 255, 24. doi:10.3847/1538-4365/ac0893, arXiv:2103.12102.
- Villar, V.A., Hosseinzadeh, G., Berger, E., et al., 2020. SuperRAENN: A Semisupervised Supernova Photometric Classification Pipeline Trained on Pan-STARRS1 Medium-Deep Survey Supernovae. *ApJ* 905, 94. doi:10.3847/1538-4357/abc6fd, arXiv:2008.04921.

Watson, C.L., Henden, A.A., Price, A., 2006. The International Variable Star Index (VSX). Society for Astronomical Sciences Annual Symposium 25, 47.

Wenger, M., Ochsenbein, F., Egret, D., et al., 2000. The SIMBAD astronomical database. The CDS reference database for astronomical objects. Astronomy and Astrophysics Supplements 143, 9–22. doi:10.1051/aas:2000332, arXiv:astro-ph/0002110.

Appendix A. ZTF DR4 light curves

Light curves of 11 newly found transients, generated with the ZTF SNAD viewer. The plots show only data from ZTF DR4 used for feature extraction (Section 2.4).

Appendix B. Light-curve features

We extract 41 light-curve features for each of $zg-$ and $zr-$ passbands using the `light-curve-feature` Rust crate (Malanchev et al., 2021)¹⁵. We use the following feature extractors:

- a magnitude amplitude;
- a magnitude standard deviation;
- kurtosis of magnitude and flux distributions, two features;
- skews of magnitude and flux distributions, two features;
- Anderson–Darling test of normality statistics values for magnitudes and fluxes, two features;
- a fraction of observations beyond one/two standard deviations from mean magnitude (D’Isanto et al., 2016), two features;
- a range of cumulative sums of magnitudes and fluxes (Kim et al., 2014), two features;

¹⁵See detailed feature description and package documentation on <https://docs.rs/light-curve-feature/0.2.2/>

- a magnitude inter-percentile ranges 2% – 98%, 10% – 90% and 25% – 75%, three features;
- a slope and its error of a linear fit of a magnitude light curve with and without respect to the observation errors, four features;
- a ratio of magnitude inter-percentile ranges: 1) 40% – 60% to 5% – 95% and 2) 20% – 80% to 5% – 95% (D’Isanto et al., 2016), two features;
- a mean magnitude value with and without respect to the observation errors, two features;
- a median of the absolute value of the difference between magnitude and median of magnitude distribution (D’Isanto et al., 2016);
- a fraction of observations being within 0.1/0.2 magnitude amplitude from median magnitude (D’Isanto et al., 2016), two features;
- the maximum deviation of magnitude from median magnitude (D’Isanto et al., 2016);
- a ratio of 5% – 95%/10% – 90% magnitude inter-percentile range to the median magnitude (D’Isanto et al., 2016), two features;
- signal-to-noise ratio of five largest Lomb–Scargle periodogram peaks, periodogram power standard deviation, and a fraction of periodogram points beyond two/three standard deviations from the mean power value, (Lomb, 1976b; Scargle, 1982b; D’Isanto et al., 2016), eight features;
- the Stetson K coefficient for magnitudes and fluxes (Stetson, 1996), two features;
- an excess variance of fluxes (Sánchez et al., 2017),
- a ratio of flux standard deviation to its mean.

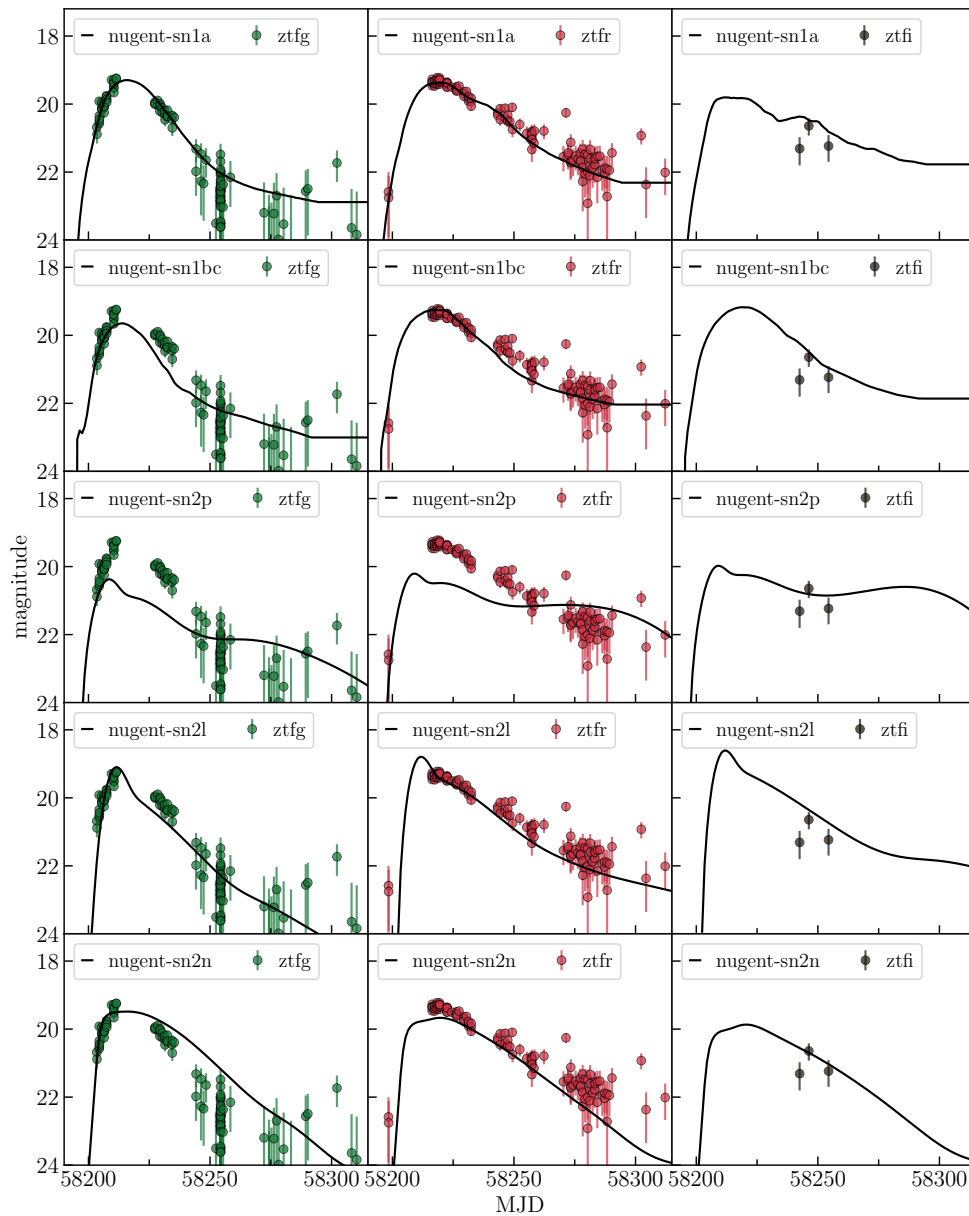


Figure 2: Results of light curve fit of SNAD150 by Nugent's supernova models. Observational data correspond to OIDs: 679108100003227 (*zg*), 679208100014706 (*zr*), 679308100021192 (*zi*).

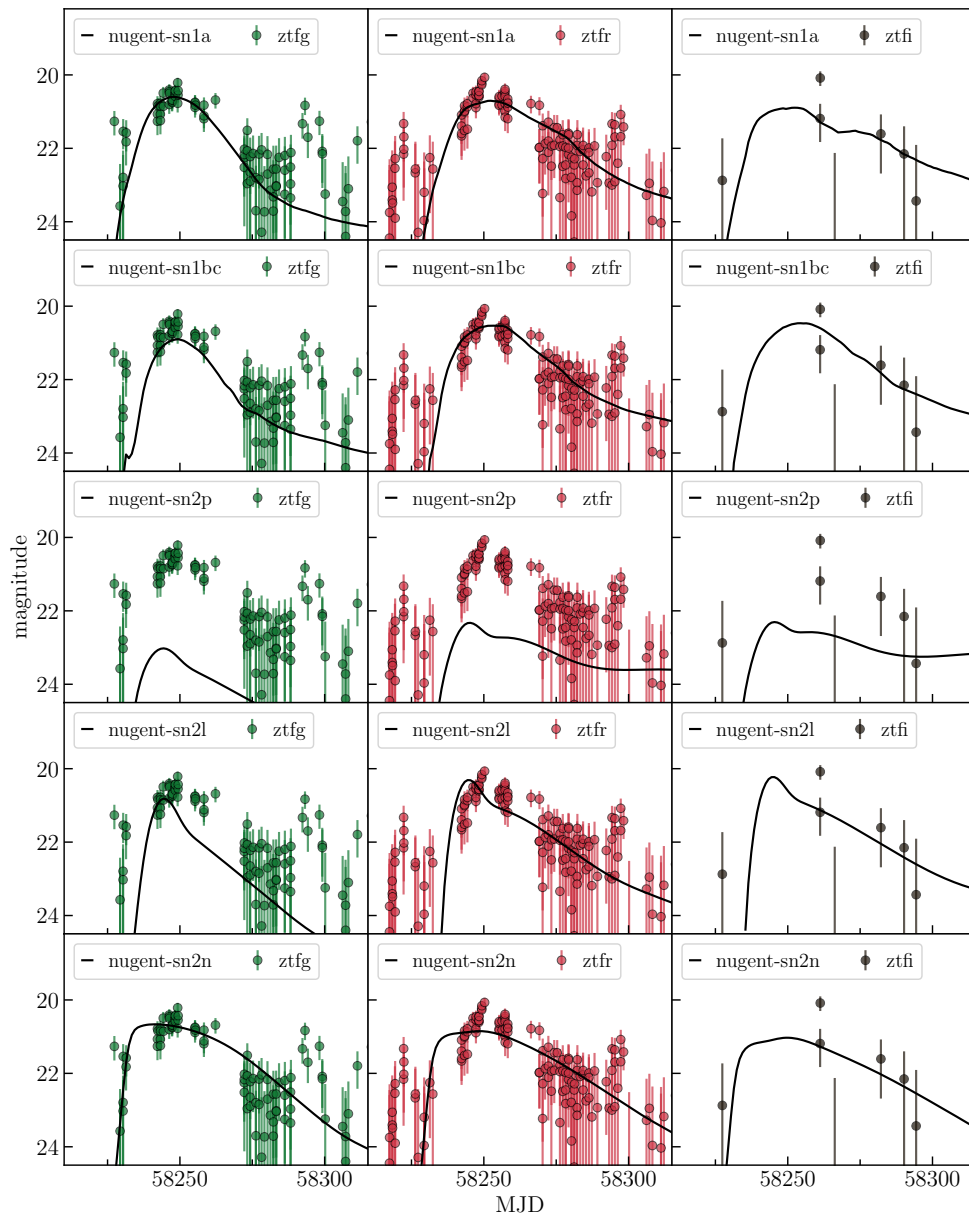


Figure 3: Results of light curve fit of SNAD154 by Nugent's supernova models. Observational data correspond to OIDs: 719102100006086 (*zg*), 719202100004008 (*zr*), 719302100018848 (*zi*).

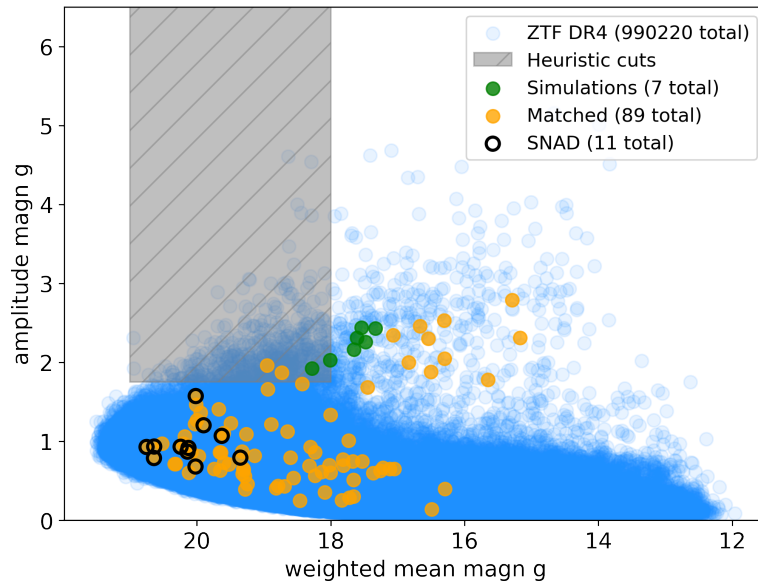
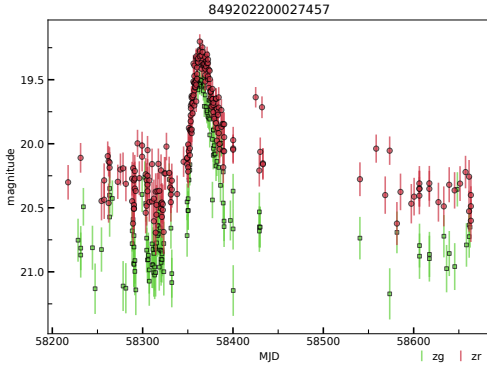
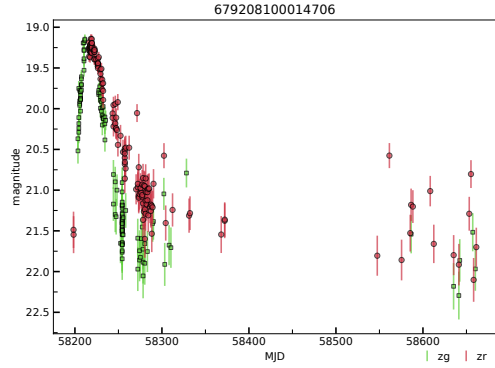


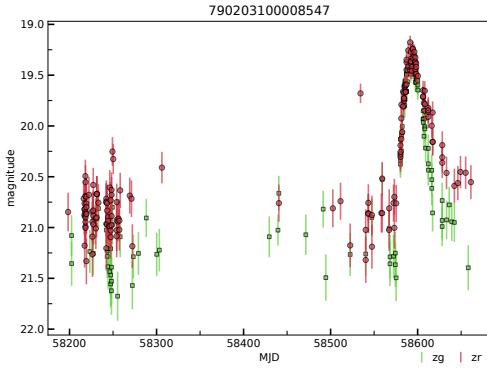
Figure 4: A scatterplot of two light curve features (zg - *error-weighted mean magnitude* and zg - *magnitude amplitude*) of all ZTF DR4 sources considered in this work (blue circles), simulations used as input to the k-D tree (green circles), uniquely matched ZTF DR4 sources (yellow circles), and those unique sources which constitute our new SNAD transients (outer black circles). We show a hatched region of our heuristic cuts from Sec. 4.2, highlighting that none of our new SNAD transients could be found with simple data quality cuts.



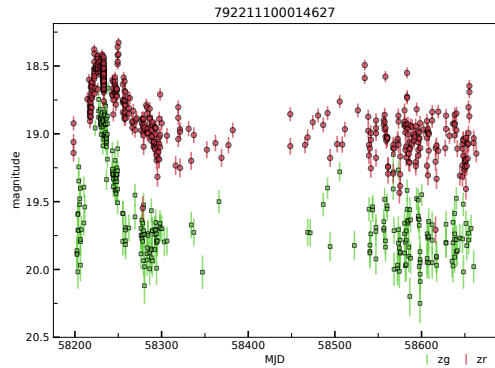
a) SNAD149: 849102200015533 (*zg*),
849202200027457 (*zr*)



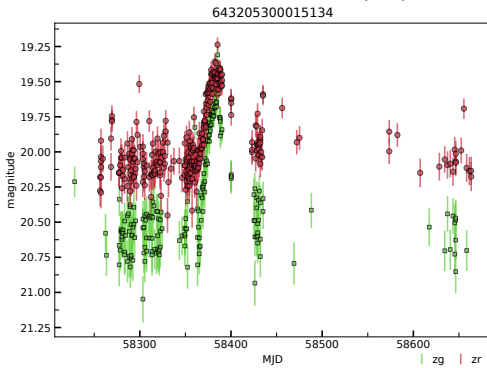
b) SNAD150: 679108100003227 (*zg*),
679208100014706 (*zr*)



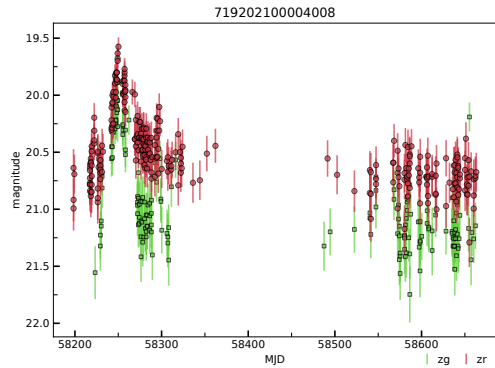
c) SNAD151: 790103100000915 (*zg*),
790203100008547 (*zr*),
1792109200005099 (*zg*)



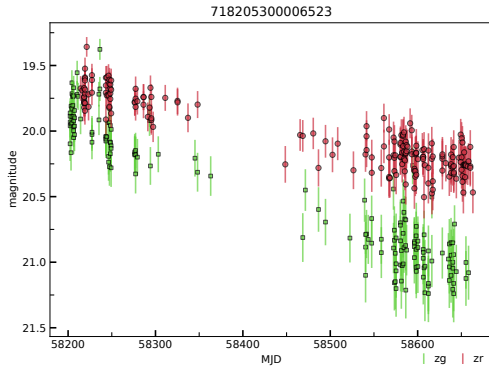
d) SNAD152: 792111100012457 (*zg*),
792211100014627 (*zr*)



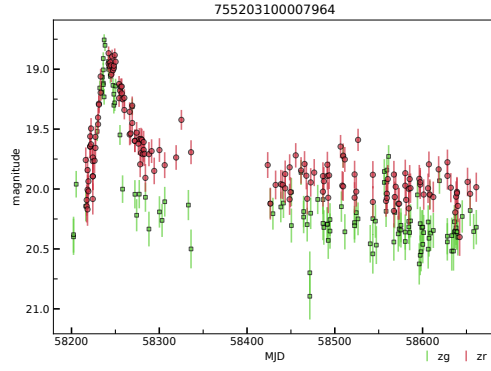
e) SNAD153: 643105300009229 (*zg*),
643205300015134 (*zr*)



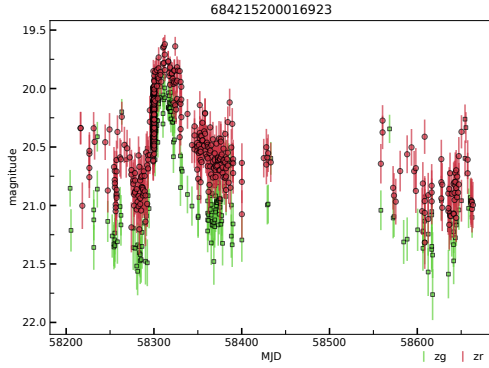
f) SNAD154: 719102100006086 (*zg*),
719202100004008 (*zr*)



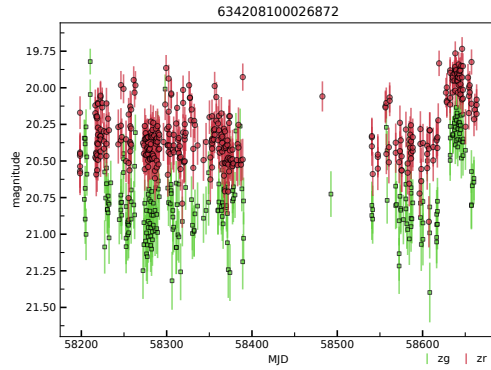
g) SNAD155: 718105300007353 (*zr*),
718205300006523 (*zg*),
1717111100000191 (*zr*)



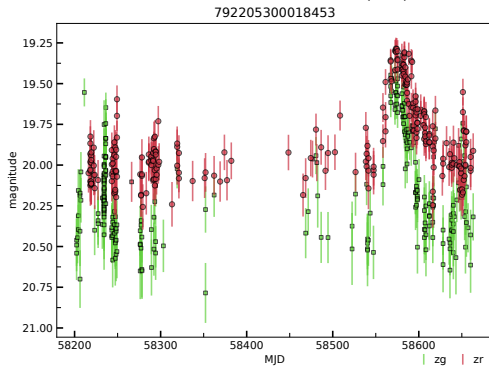
h) SNAD156: 755103100026105 (*zg*),
755203100007964 (*zr*)



i) SNAD157: 684115200018744 (*zg*),
684215200016923 (*zr*),
1725206200027715 (*zr*)



j) SNAD158: 634108100006647 (*zg*),
634208100026872 (*zr*)



k) SNAD159: 792105300007593 (*zg*),
792205300018453 (*zr*),
1795111100013935 (*zg*),
1795211100000534 (*zr*)

Figure A.5: SN/AGN candidate light curves in *zr*- and *zg*-bands within the first 420 days of ZTF DR4, generated with the ZTF SNAD viewer.